Conformational changes in matrix-isolated 6-methoxyindole: Effects of the thermal and infrared light excitations

Q1 A. J. Lopes Jesus,[1,2] I. Reva,[1,a)] C. Araujo-Andrade,[1,3,4] and R. Fausto[1]
[1]*CQC, Department of Chemistry, University of Coimbra, 3004-535 Coimbra, Portugal*
[2]*CQC, Faculty of Pharmacy, University of Coimbra, 3004-295 Coimbra, Portugal*
[3]*Unidad Académica de Física de la Universidad Autónoma de Zacatecas, Zacatecas, Mexico*
[4]*ICFO–The Institute of Photonic Sciences, 08860 Castelldefels (Barcelona), Spain*

(Received 11 January 2016; accepted 7 March 2016; published online XX XX XXXX)

Conformational changes induced thermally or upon infrared excitation of matrix-isolated 6-methoxyindole were investigated. Narrowband near-infrared excitation of the first overtone of the N–H stretching vibration of each one of the two identified conformers is found to induce a selective large-scale conversion of the pumped conformer into the other one. This easily controllable bidirectional process consists in the intramolecular reorientation of the methoxy group and allowed a full assignment of the infrared spectra of the two conformers. Matrices with different conformational compositions prepared by narrow-band irradiations were subsequently used to investigate the effects of both thermal and broadband infrared excitations on the conformational mixtures. Particular attention is given to the influence of the matrix medium (Ar vs. Xe) and conformational effects of exposition of the sample to the spectrometer light source during the measurements. © *2016 AIP Publishing LLC.* [http://dx.doi.org/10.1063/1.4944528]

I. INTRODUCTION

Isolating molecular species in low-temperature solid matrices of inert gases is nowadays a well-established experimental technique used to characterize and control the conformational population of isolated molecules.[1–4] Two methodologies are commonly employed to alter the relative abundance of the trapped conformers: annealing of the sample[5,6] or subjecting it to narrowband or broadband radiation of the IR or UV spectral regions.[2,7–14] In the first case, the population of less stable forms is reduced in ~~favour~~ of the most stable ones, providing that the energy barriers for the isomerizations can be surmounted. In the second case, the conformational interconversions may occur in both directions, thus permitting population and stabilization of very high energy conformers, which otherwise would be rather difficult to be experimentally detected.[4,14,15]

Very recently, we have investigated the conformational changes in matrix-isolated 6-methoxyindole (6MOI) induced by narrowband near-IR (NIR) excitation.[2] Using monochromatic laser radiation tuned at the frequency characteristic of the first NH stretching overtones of the two identified conformers (see their geometries in Figure 1), we were able to selectively shift the conformational composition in both directions. Especially relevant in this isomerization is the fact that the rotating methoxy fragment and the excited NH group stay remote from one another (both are separated by four covalent bonds). Such remote infrared-induced isomerizations were observed previously by ultrafast spectroscopy in the gas phase.[16–20] In matrices, however, vibrationally induced conformational manipulation of remote groups is still very uncommon. To the best of our knowledge, in such experimental conditions, the only remote conformational interconversion triggered by selective NIR excitation has been reported by Halasa *et al.*, for the S–H rotamerization in 2-thiocytosine induced by NIR selective excitation of the NH_2 stretching overtone.[21]

In this work, we explore different strategies of modifying the conformational distribution of 6MOI isolated in low-temperature argon and xenon matrices. Therefore, after identifying and characterizing the two conformers of the molecule by infrared spectroscopy, changes on their relative populations were induced by annealing, as well as by broadband and narrowband NIR/mid-IR irradiation. It is important to point out that up to date, most of the studies about conformational isomerizations resulting from NIR/mid-IR excitations of matrix-isolated molecules involved the rotation of light OH (more frequently observed)[3,4,22,23] or SH groups.[21] On the other hand, in previous studies of molecules with conformers differing from each other by rotation of bulky fragments (such as OCH_3 or OCOH), no isomerizations have been observed after subjecting the matrices to broadband or narrowband IR radiation.[23–25]

From a wider perspective, the results obtained in this work provide basic knowledge that can be used to understand local conformational features in many relevant methoxyindole-containing naturally occurring and synthetic biomolecules.[26–30] Also, the possibility of controlling the conformational distribution of 6MOI in matrices opens a window for exploiting its conformer-specific reactivity in condensed media (as opposite to the gas phase). In addition, this work also demonstrates in a very clear way that exposition of a conformationally flexible sample to the broadband

a)Author to whom correspondence should be addressed. Electronic mail: reva@qui.uc.pt

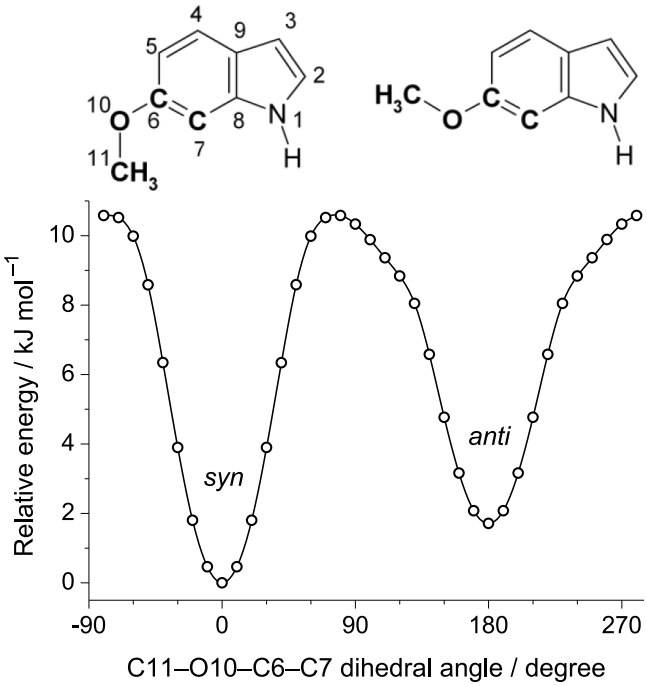

FIG. 1. Relaxed potential energy scan of 6MOI as function of the internal rotation of the O–CH_3 group calculated at the B3LYP/6-311++G(d,p) level of theory. The numbering scheme of heavy atoms is indicated for the most stable *syn* conformer, whose electronic energy was chosen as relative zero.

infrared beam of an infrared spectrometer might substantially influence the obtained results due to occurrence of *a priori* unexpected IR-induced isomerization processes and also might be observed by stationary spectroscopic techniques.

II. COMPUTATIONAL SECTION

The minimum energy conformations of 6MOI were first identified through a potential energy scan, at the B3LYP/6-311++G(d,p) level of theory, around the C11–O10–C6–C7 dihedral angle, Figure 1. This dihedral was varied from 0 to 360°, with increments of 10°. At each scanning point, all the remaining internal coordinates were allowed to relax. The located minima were then fully optimized with the same B3LYP[31–33] functional and the MP2 (second-order Møller-Plesset) method,[34] both combined with the 6-311++G(d,p) and 6-311++G(3df,3pd) basis sets. The respective Cartesian coordinates are provided in Table S1 of the supplementary material.[43] Harmonic B3LYP vibrational calculations were conducted on the geometries optimized at the same level. This allowed calculating the zero-point vibrational energy (ZPVE), as well as the thermal and entropic energy corrections, both evaluated at 323 K (temperature of the vapours of the compound before the matrix deposition, see below). Through these calculations, it was also possible to obtain the theoretical vibrational frequencies and infrared intensities that are listed in Table S2 of the supplementary material.[43] To correct for the systematic shortcomings of the applied methodology (vibrational anharmonicity, basis set truncation, and the neglected part of electron correlation) and for the matrix shifts, two multiplicative factors were used to scale the calculated B3LYP/6-311++G(d,p) harmonic vibrational frequencies: 0.95 above 3300 cm^{-1} (for the NH stretching modes) and 0.98 below 3300 cm^{-1} (for the remaining modes). All quantum-mechanical computations referred above were carried out with the Gaussian 09 program package.[35]

III. EXPERIMENTAL SECTION

Commercial 6MOI, supplied by Apollo Scientific (98% purity), has been used in the matrix isolation experiments. A few milligrams of the solid compound was placed inside a miniature glass oven which was then assembled inside the vacuum chamber of a cryostat, constituted by an APD cryogenics closed-cycle helium refrigerator system with a DE-202A expander. Argon and xenon matrices were prepared by co-deposition of vapors of the compound coming out from the oven (resistively heated up to ~323 K) with an excess of the host gas (argon N60 and xenon N48, both supplied by Air Liquide) onto a CsI optical substrate, which was cooled to 16 and 20 K during deposition of 6MOI into argon and xenon matrices, respectively. The temperature of the CsI window was measured directly at the sample holder with an accuracy of 0.1 K by using a silicon diode sensor connected to a digital controller (Scientific Instruments, Model 9650-1).

In order to monitor the deposition process and to follow the conformational changes occurring in the matrices, mid-infrared spectra (4000–400 cm^{-1}) were collected using a Thermo Nicolet 6700 Fourier-transform infrared (FTIR) spectrometer equipped with a Ge/KBr beam splitter and a mercury cadmium telluride (MCT-B) detector, cooled by liquid N_2. All mid-IR spectra were collected with a resolution of 0.5 cm^{-1}. In the near-infrared range, the spectra were recorded with a resolution of 1 cm^{-1}, using a CaF_2 beam splitter and the same MCT-B detector. Narrowband frequency-tunable NIR light provided by the idler beam of a Quanta-Ray MOPO-SL optical parametric oscillator pumped with a pulsed Nd:YAG laser (pulse energy 10 mJ, duration 10 ns, repetition rate 10 Hz), was used to irradiate the matrices. In some experiments, a standard Edmund Optics long-pass filter was used (transmission cutoff value of ~4.50 μm) to protect the matrices from light with wavenumbers above 2200 cm^{-1}.

IV. RESULTS AND DISCUSSION

A. Gas phase conformational equilibrium

Two minimum energy conformations are identified from the potential energy scan displayed in Figure 1. Both have the heavy atoms of methoxy group lying in the same plane of the indole ring (C_s symmetry). This maximizes the conjugation between the electron lone-pairs of the oxygen atom and the π-system of the aromatic ring.[36] Following the nomenclature adopted by Brand *et al.*,[37] the conformer with α = 0° is designated as *syn*, while that with α = 180° is called *anti*. In the first case, the OCH_3 and NH groups are pointing in the same direction, while in the second they are pointing in opposite directions. The geometries of both conformers are shown in Figure 1, while their relative electronic energies (ΔE_{elec}),

TABLE I. Relative electronic (ΔE_{elec}), zero-point corrected (ΔE_0), and Gibbs (ΔG) energies at 323 K (kJ mol^{-1}) for the two 6MOI conformers and their Boltzmann populations estimated at the same temperature (pop., %).

	Conformer	
Level of theory	*Syn*	*anti*
B3LYP[a]		
ΔE_{elec}	0.00/0.00	1.78/1.93
ΔE_0	0.00/0.00	1.72/1.76
ΔG (323 K)	0.00/0.00	1.14/1.20
Pop. (323 K)[b]	60.4/61.0	39.6/39.0
MP2[a,c]		
ΔE_{elec}	0.00/0.00	3.17/2.90
ΔE_0	0.00/0.00	3.11/2.74
ΔG (323 K)	0.00/0.00	2.53/2.18
Pop. (323 K)[b]	72.0/69.2	28.0/30.8
CC2/cc-pVTZ[d]		
ΔE_{elec}	0.00	3.23
ΔE_0	0.00	2.98
Pop. (323 K)[e]	75.2	24.8

[a]Values on the left hand-side of the slash were obtained with the 6-311++G(d,p) basis set, while those on the right hand-side were obtained with the 6-311++G(3df,3pd) basis set.
[b]Estimated from the Gibbs energy values.
[c]The ZPVE as well as the thermal and entropic corrections at 323 K added to the MP2 electronic energies was calculated at the B3LYP level.
[d]Taken from Ref. 37.
[e]Estimated from the relative zero-point corrected energies (ΔE_0).

zero-point corrected energies (ΔE_0, $E_0 = E_{elec} + \text{ZPVE}$), and Gibbs energies ($\Delta G$) at 323 K (temperature of the gaseous samples prior to the matrix deposition), predicted at different levels of theory, are given in Table I. This table shows also the predicted Boltzmann populations of the two forms at 323 K.

Q3 At the B3LYP level of theory, *syn* is the lowest energy conformer with *anti* being 1.8 or 1.9 kJ mol^{-1} higher in energy, depending on if this functional is combined with the 6-311++G(d,p) or 6-311++G(3df,3pd) basis sets, respectively. Optimizations with the MP2 method do not alter the energetic order of the two conformers, though their energy difference increases to ~3 kJ mol^{-1}. This MP2 energy difference is very close to that computed with the approximate coupled cluster single and doubles model (CC2) combined with the cc-pVTZ basis set, 3.2 kJ mol^{-1}.[37] Adding the ZPVE, as well as the thermal and entropic corrections to the electronic energies, the Gibbs energy difference between the two forms at 323 K is reduced to ~1.2 kJ mol^{-1} (DFT (density functional theory)) and to 2.2–2.5 kJ mol^{-1} (MP2). It follows that the predicted equilibrium abundances of the *anti* and *syn* forms at this temperature are, respectively, ~60%: ~40% at the DFT level and ~70%: ~30% at the MP2 level. Again, these values are similar to those obtained from the zero-point corrected CC2-energies.[37] Q4

Based on these predictions, the two conformers should be present in the gaseous sample of 6MOI before the matrix deposition. Since they are separated by a medium-high energy barrier (~9 kJ mol^{-1} in the *anti* → *syn* direction, see Figure 1), no conformational cooling[5,6,38,39] is expected to occur during the deposition, and therefore both of them should be preserved in both matrices immediately after the deposition, as it has already been confirmed in our previous experiments.[2]

B. Interpretation of the mid-IR spectra

Figure 2 shows the mid-infrared spectra of 6MOI isolated in an argon (Fig. 2(a)) and a xenon (Fig. 2(b)) matrix, measured immediately after the matrix deposition. We shall call them for brevity "Ar spectrum" and "Xe spectrum" hereafter. Approximate descriptions of the vibrations assigned to the experimental bands are presented in Table II.

At a glance, there is no appreciable difference between both experimental spectra. The only notable exception is the profile of the spectral feature located at the 3550-3450 cm^{-1} interval, which is assigned to the stretching vibration of the NH group (νNH). For 6MOI in xenon matrix, this absorption has a doublet profile with two well-defined components at 3498 and 3494 cm^{-1}.[2] In the case of the argon matrix, this band is split into seven sub-bands, with the most prominent ones located

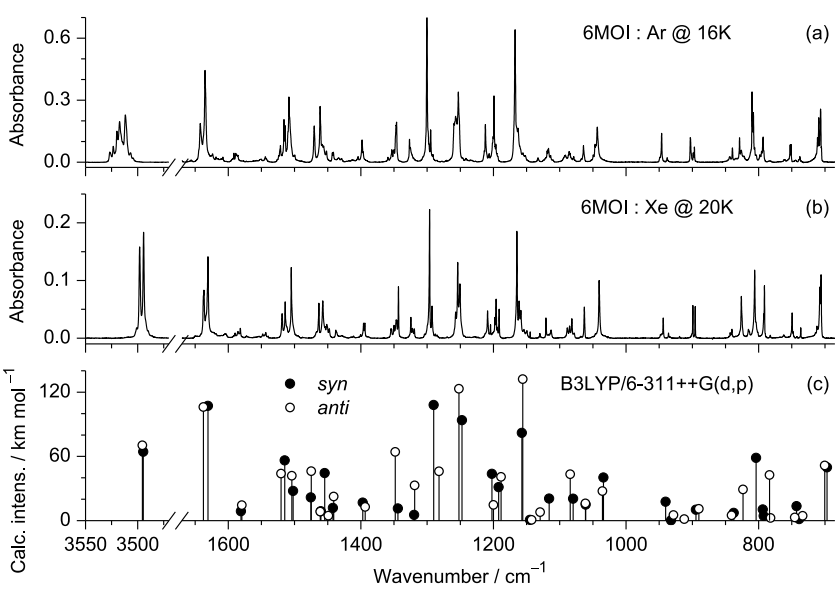

FIG. 2. Experimental mid-IR spectra recorded immediately after deposition of 6MOI in low-temperature Ar (a) and Xe (b) matrices, and (c) theoretical spectra of the *syn* (closed circles) and *anti* (open circles) conformers calculated at the B3LYP/6-311++G(d,p) level of theory. The computed wavenumbers above and below 3300 cm^{-1} were multiplied by 0.95 and 0.98, respectively.

TABLE II. Experimental and calculated [B3LYP/6-311++G(d,p)] wavenumbers ($\tilde{\nu}$, cm^{-1}) and calculated infrared intensities (I, km mol^{-1}) for the isolated 6MOI molecule.

Experimental[a]		Calculated[b]					
		syn		*anti*			
Xe, 20 K	Ar, 16 K	$\tilde{\nu}$	I	$\tilde{\nu}$	I	Sym.	Approximate description[c]
3498 (s)[d]	3512 (m)			3491.8	70.4	A′	νNH
3494 (vs)[d]	3520/3517 (w) 3507 (vw)	3490.9	64.3			A′	νNH
1637 (w)[d]	1642 (w)[d]			1637.5	106.1	A′	νCC_{benz}
1631 (s)[d]	1635 (s)[d]	1630.5	107.1			A′	νCC_{benz}
1519 (w)[d]	1521 (vw)[d]			1520.4	43.9	A′	νC2C3
1514 (w)[d]	1516* (w)[d]	1514.9	56.2			A′	νC2C3
1505 (s)	1508 (m)	1502.2	27.7	1504.1	42.0	A′	δC5H + δNH + νCC
1463 (m)	1470 (w)	1475.4	21.6	1474.9	46.2	A′	δCH_3 as
1457 (w)	1462 (w)	1454.2	44.4			A′	δC4H + δC7H + C2H
1437 (vw)	1442 (vw)	1442.1	11.8	1440.9	22.4	A′	δCH_3 s
1396 (vw)	1398 (vw)	1397.0	16.9			A′	$\nu C2N + \delta NH + \delta CH_{py}$
1394 (vw)	1396 (vw)			1393.5	12.8	A′	$\nu C2N + \delta NH + \delta CH_{py}$
1343* (m)	1346* (w)	1344.1	11.3	1348.2	64.2	A′	δC5H + δNH
1325* (w)	1327 (vw)	1319.6	5.3	1318.9	32.9	A′	δCH + νCC
1296 (vs)[d]	1300 (vs)[d]	1290.2	108.0			A′	νC6O + νC8N + νCC
1293 (w)[d]	1295 (w)[d]			1282.1	46.1	A′	νC6O + νC8N + νCC
1254* (s)	1257 (m)			1252.1	123.1	A′	δCH
1251 (m)	1253 (m)	1247.5	93.8			A′	δCH
1209/1204 (w)	1212 (w)	1202.3	43.7	1199.9	14.6	A′	δCH
1196/1191 (w)	1199 (m)	1192.1	31.2	1188.5	40.9	A′	ρCH_3
1165* (vs)	1167 (vs)	1157.2	82.0	1155.8	132.2	A′	$\rho CH_3 + \delta C7H + \delta NH$
1130 (vw)	1133 (vw)			1129.6	7.9	A′	δC4H + δC5H
1121/1113 (vw)	1117* (vw)	1115.9	20.6			A′	δC4H + δC5H
1082* (w)	1086* (vw)	1079.8	20.5	1084.1	43.3	A′	δC2H
1063 (w)	1064 (vw)	1060.8	14.9	1061.3	16.1	A′	δC3H
1041 (m)	1043* (w)	1034.0	40.3	1035.6	27.6	A′	νC11O + δC7H
944 (vw)	946 (w)	940.3	17.6			A′	δ benz
936 (vw)	938 (vw)			928.4	5.2	A′	δ benz
899 (w)[d]	903 (w)[d]	894.6	10.2			A′	δ py
896 (w)[d]	897* (vw)[d]			890.2	11.0	A′	δ py
843 (vw)	844 (vw)			840.8	5.0	A″	γC2H + γC3H iop
840 (vw)	839 (vw)	837.5	7.3			A″	γC2H + γC3H iop
826 (w)	829 (w)			823.5	29.1	A″	γC7H
806 (m)[d]	810* (m)[d]	803.8	58.6			A″	γC4H + γC5H isp
791 (s)[d]	793 (w)[d]			783.7	42.6	A″	γC4H + γC5H isp
749* (vw)	752* (vw)	742.7	13.4	745.4	3.0	A″	γ ind
737 (vw)	738 (vw)			733.6	4.5	A′	δ benz
712/708 (m)	711/709 (w)	696.8	49.8			A″	γC2H + γC3H isp
706 (m)	707* (m)			700.3	51.5	A″	γC2H + γC3H isp

[a]Experimental intensities are expressed in a qualitative way: vs = very strong; s = strong; m = medium; w = weak; vw = very weak. Some of the absorptions with very low intensity, as well as those falling in the 3150–2800 cm^{-1} region (CH and CH_3 stretching vibrations) and below 700 cm^{-1} are not shown. For some split bands (denoted by an asterisk), only the most intense components are shown.

[b]Calculated harmonic wavenumbers are scaled by 0.95 and 0.98, above and below 3300 cm^{-1}, respectively. The assignment of the experimental absorptions to a specific conformer was based on the direct comparison between the calculated and experimental bands and on the spectral changes induced by the thermal and NIR excitations.

[c]Carried out by ChemCraft animation of the vibrations of the *syn* and *anti* conformers. Abbreviations: ν, stretching; δ, in-plane deformation; γ, out-of-plane deformation; ρ, rocking; s, symmetric; as, antisymmetric; isp, in the same phase; iop, in the opposite phase; ind, indole ring; py, pyrrole fragment; benz, benzene fragment.

[d]Pairs of bands used to estimate the conformational populations.

near 3512, 3517, and 3520 cm^{-1} (see Figure 3(b) for details). Since 6MOI possesses only two conformers that could be stabilized in the solid matrices, and each of them gives rise to only one transition in this spectral range (NH stretching), the more complex pattern exhibited by this absorption in the Ar spectrum must be due to the existence of different trapping sites in this matrix host, which gives rise to a number of closely located IR peaks. An attempt to assign these trapping

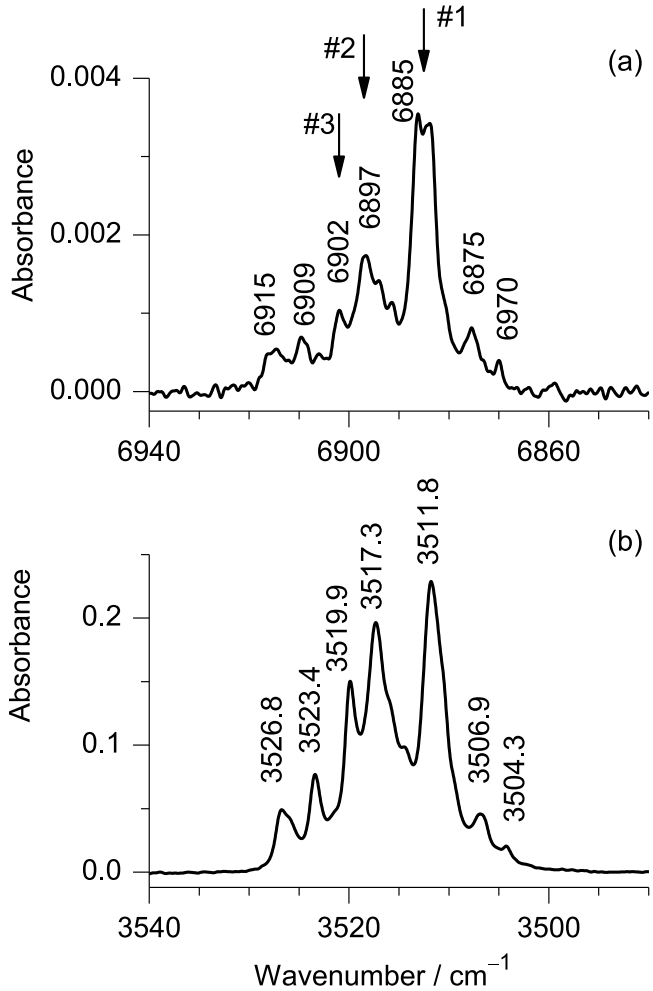

FIG. 3. Fragments of the near-IR (a) and mid-IR (b) spectrum of 6MOI isolated in solid argon at 16 K showing the multiplet profiles of the absorption bands due to the 2νNH overtone transition and νNH fundamental transition. The numbered vertical arrows show the positions of the near-IR irradiations, whose effects are depicted in Figure 4.

sites to different conformers is described below, where the results of the monochromatic NIR irradiations were taken into account.

Comparing now the mid-IR experimental spectra with those calculated for the two conformers (Figure 2(c)), it becomes evident that both forms are stabilized in the matrix. As a matter of fact, some of the doublets found in the experimental spectra, such as those located in the 3498–3494 cm^{-1} (νNH, only in Xe), 1645–1630 cm^{-1} (νCC$_{benz}$), 1521–1514 (νC2C3), 1300–1293 cm^{-1} (νC6O + νC8N + νCC), 1257–1251 cm^{-1} (δCH), 903–896 cm^{-1} (δ$_{py}$) regions, correspond, in the calculated spectra, to pairs of vibrations of both conformers. In the 840–780 cm^{-1} region, it is also possible for discriminating band characteristic of both conformers. Indeed, those at 826(Xe)/829(Ar) cm^{-1} (γC7H) and 791/793 cm^{-1} (γC4H + γC5H isp) are with no doubt assigned to the less stable conformer, while the middle one centred at 806/810 cm^{-1} (γC4H + γC5H iop) corresponds to the most stable form. Based on this comparison and on the spectral modifications observed upon annealing and NIR irradiations (see discussion below),[2] some of the experimental bands can be reliably assigned to a specific conformer, as shown in Table II.

In quantitative terms, the populations (P) of the two matrix-isolated conformers can be estimated from the integrated absorbances (A) of different doublet bands, each one of the components assigned to a different conformer, normalized by the corresponding calculated intensities (I): $P_{syn}/P_{anti} = (A_{syn}/A_{anti}) \times (I_{anti}/I_{syn})$. Six pairs of bands of the Xe spectrum and five of the Ar spectrum, which are indicated in Table II, were used to estimate the populations. The following mean values (±standard deviation) were obtained: Xe, $P_{syn}/P_{anti} = 1.5 \pm 0.2$ (59%:41%); Ar, $P_{syn}/P_{anti} = 2.0 \pm 0.1$ (67%:33%). It is worth noticing that according to these estimations, the conformational composition in solid xenon is more shifted towards the less stable rotamer than in argon. In addition, it is also interesting to see that the results obtained in argon are close to the MP2-predicted gas-phase populations, while those found in xenon are in excellent agreement with the B3LYP predictions. The above population ratio of 6MOI conformers observed in xenon matrix results from a fortuitous coincidence with the B3LYP prediction. The true reasons can be understood by a deep analysis of the photo- and thermally induced isomerizations occurring in both matrices, as described in detail below.

C. Narrowband near-IR excitations

As referred in the Introduction, we have previously demonstrated that the two conformers of 6MOI can be converted into one another by exposing the matrix to monochromatic NIR laser-light tuned at the frequency of the respective first NH stretching overtone (2νNH).[2] In the case of the Xe matrix, these 2νNH absorptions have been identified at 6855.6 and 6849.3 cm^{-1} for the *anti* and *syn* conformers, respectively, with the νNH counterparts at 3498.0 and 3494.5 cm^{-1} in the fundamental region. A large-scale *syn* → *anti* transformation was detected upon irradiation at 6849 cm^{-1}, while the reverse process could be also induced by tuning the laser light at 6856 cm^{-1}.

Concerning the spectrum recorded in Ar matrix, the multiplet profile of the 2νNH (Figure 3(a)) and νNH (Figure 3(b)) absorptions requires a more careful analysis in order to assign the band components in these regions to a specific conformer. NIR excitations were carried out at wavenumbers corresponding to different maxima within the 2νNH profile. Their positions are designated by numbered vertical arrows in Figure 3(a). The outcome of these irradiations was monitored through the spectral variations occurring in the 3530–3500 cm^{-1} and 1650–1625 cm^{-1} mid-IR regions, Figure 4. The latter region is shown as a reference, because it contains a doublet band where the higher and lower frequency components are unequivocally assigned to the *anti* and *syn* conformers, respectively (see Table II).

The NIR irradiations were initiated by tuning the laser at the position of the most intense 2νNH peak: 6885 cm^{-1} (see arrow #1 in Fig. 3(a)). The intensity variations observed in the doublet band at 1642/1635 cm^{-1} (Fig. 4(b), right), as well as in the other pairs of bands in the mid-IR range, unmistakably reveal the existence of an *anti* → *syn* conversion. Based on this

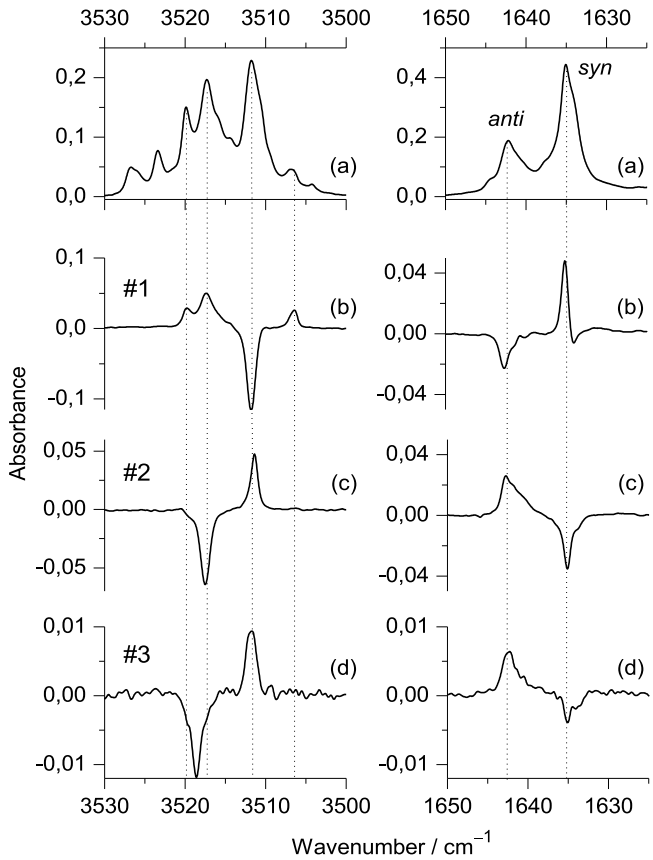

FIG. 4. Representation of the 3530–3500 cm^{-1} ((a), left) and 1650–1625 cm^{-1} ((a), right) regions of the mid-IR spectrum of 6MOI isolated in solid argon at 16 K, and spectral changes in these regions after narrowband NIR irradiations #1 at 6885 cm^{-1} (b), #2 at 6897 cm^{-1} (c), and #3 at 6902 cm^{-1} (d) (see Figure 3). These changes are shown in frames ((b)-(d)) and correspond to difference spectra obtained by subtracting the spectrum recorded after the irradiation from that measured before the irradiation. Positive bands in frames ((b)-(d)) correspond to those growing up during the irradiations.

result, one can assign the most intense νNH band component located near 3512 cm^{-1} to the *anti* conformer and those near 3520, 3517, and 3506 cm^{-1} (which grow up under these experimental conditions) to the *syn* conformer trapped into three different matrix sites.[40] The next irradiation was carried out at 6897 cm^{-1} (arrow #2 in Fig. 3(a)) and led to the opposite conformational conversion (Fig. 4(c)). Note that in this case, only the *syn* conformers trapped into the most populated site (identified by the peak near 3517 cm^{-1}) were converted to *anti*, while those trapped into the less abundant sites (identified by the peaks near 3520 and 3506 cm^{-1}, Fig. 3(b)) remained unchanged. A similar *syn* → *anti* transformation (Fig. 4(d)), though much less effective, was induced by a NIR excitation at 6902 cm^{-1} (arrow #3 in Fig. 3(a)). In an attempt to excite the conformers trapped into the sites responsible for the peaks near 3527 and 3523 cm^{-1}, we have conducted excitations at the corresponding overtones: 6915 and 6909 cm^{-1} (see the highest-frequency components in Figures 3(a) and 3(b)). However, no significant spectral changes were detected, which was taken as an indication that the molecules trapped in these sites are not reactive.

D. Thermal annealing

Previous matrix-isolation conformational studies have been performed in methoxy-group-containing molecules with conformers differing from each other by rotation of the OCH_3 group and separated by energy barriers higher than 8 kJ mol^{-1}.[24,25,41] In all cases, no conformational relaxation was observed upon annealing the argon matrices up to the limit for the thermal stability of the host-material (~35 K). Conformational conversions were only observed after depositing some of these molecules (i.e., those with accessible energy barriers for conformational isomerization) in xenon and heating the matrices up to temperatures ranging from 30 to 55 K (~65 K is the limit for this host matrix). Based on these results, the annealing experiments in 6MOI were only conducted in xenon.

After co-deposition of 6MOI with a solid xenon host at 20 K, we have exposed the matrix-isolated compound to the monochromatic radiation of 6849 cm^{-1} in order to enrich the sample with the less stable *anti* conformer, which is expected to be consumed upon annealing. After that, the solid sample

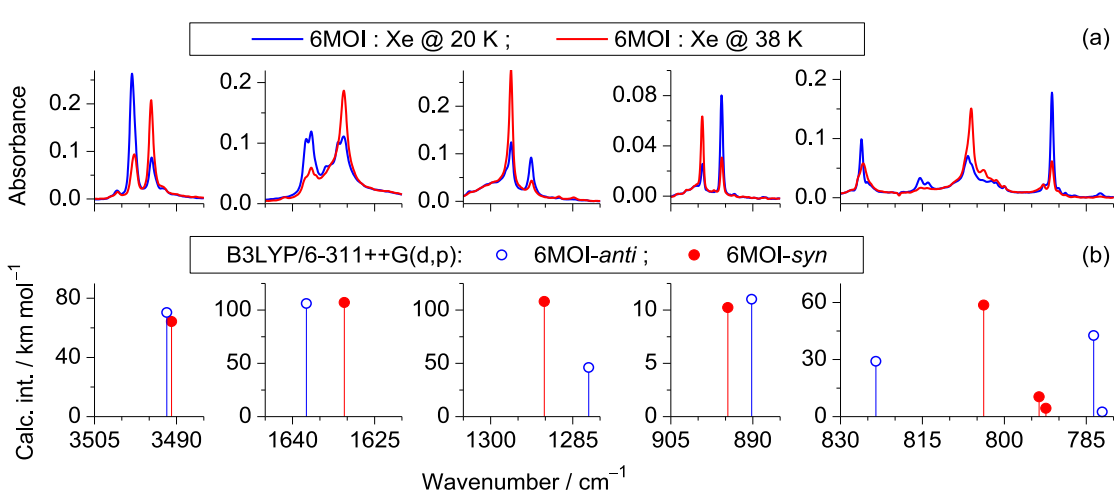

FIG. 5. (a) Selected spectral regions illustrating the changes taking place after annealing of 6MOI isolated in a Xe matrix from 20 K (red) to 38 K (blue) compared with (b) theoretical spectra of *syn* (open circles) and *anti* (closed circles) conformers of 6MOI calculated at the B3LYP/6-311++G(d,p) level of theory. Calculated harmonic wavenumbers above and below 3300 cm^{-1} were multiplied by 0.95 and 0.98, respectively.

was gradually heated with increments of 2 K. When the sample temperature reached 34 K, the intensity of the bands assigned to the *anti* conformer started to decrease, and concomitantly the bands ascribed to the *syn* form increased. These spectral changes became more pronounced after additional heating to 38 K and occurred on the time scale of a few minutes. This is well-evidenced in Figure 5, which compares selected spectral regions measured at 38 K and 30 K (a difference spectrum in the full mid-IR region is shown in Figure S1 of the supplementary material[43]). These results provide irrefutable evidence for the existence of an *anti* → *syn* relaxation, thus confirming that *syn* is in fact the most stable rotamer. In an attempt to produce the maximum possible amount of this form, we have proceeded with annealing up to 50 K. Under these conditions, it could be expected that the populations of the two conformers would shift towards those characteristic of the 50 K conformational equilibrium: $P_{syn} > 97\%$; $P_{anti} < 3\%$, values estimated from the Boltzmann distributions of the DFT and MP2 zero-point corrected energies (see Table I). In practical terms, this means that at this temperature, the less stable *anti* form should be entirely depopulated. However, despite the statistical prediction, such an equilibrium state was not achieved: the most prominent absorptions characteristic of the *anti* form were found to persist in the IR spectra measured at 50 K with a non-negligible intensity (even after letting the sample at this temperature for tens of minutes). Using the integrated intensity of the two peaks observed at 899 and 896 cm^{-1}, which are assigned to the in-plane deformation of the pyrrole ring for the *anti* and *syn* conformers, respectively, the abundance of the less stable *anti* form at 50 K was found to be ~25% (a similar estimation was obtained from other doublets). As this value is well above the predicted equilibrium population at 50 K, it can be concluded that something is shifting the conformational composition away from the equilibrium one, i.e., in the direction opposite from that triggered by temperature.

E. Effect of the broadband radiation emitted by the spectrometer source

With the objective of following the effect responsible for the non-establishment of a thermodynamic equilibrium in the Xe matrix, the annealed sample was cooled down to 30 K (in order to minimize the thermal effects) and kept at this temperature for about 2 h. During this period, various mid-IR spectra were recorded at regular time intervals. The variation of the intensity of the 899/896 cm^{-1} pair of bands shown in Figure 6(a) undoubtedly demonstrates that the most stable *syn* conformer is converted back into the less stable *anti* form. Quantitatively, after 2 h, the abundance of the *anti* conformer increased from 25% to 44%, while that of *syn* decreased from 75% to 56%, as illustrated in Figure 6(b). Interestingly, the final conformational composition (44%:56%) is very similar to that estimated from the integration of the same pair of bands in the spectrum collected immediately after the deposition of the xenon matrix at 20 K, as mentioned at the end of Section IV B. This result suggests that the conformational ratio is also affected during the matrix deposition. After keeping the sample at 30 K for two additional hours and

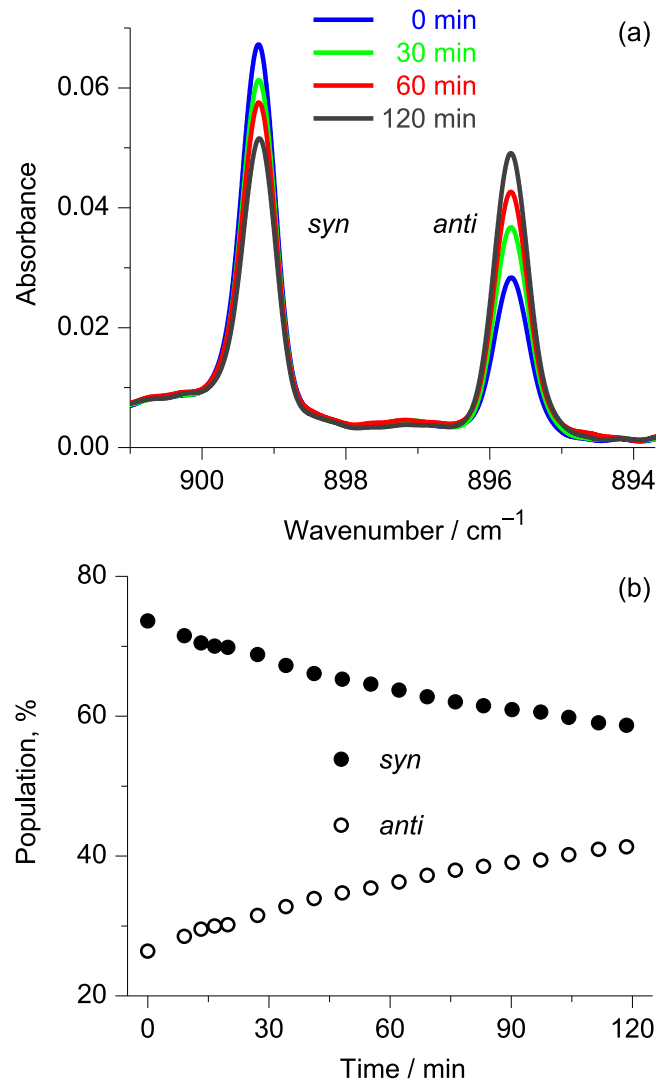

FIG. 6. (a) Intensity change of the pair of bands located in the 900–895 cm^{-1} spectral range during the permanence of 6MOI in a xenon matrix at 30 K for 2 h, after annealing the sample up to 50 K and cooling it back to 30 K; (b) variation of the population of the two conformers (obtained from the integrated intensities of the two bands) as a function of time. The initial time corresponds to the moment at which the sample was cooled back to 30 K. During recording of the spectra, the sample was exposed to the unfiltered light of the spectrometer source.

recording various spectra at the end of this period, no further changes in the populations of both conformers were detected (see Figure S2 of the supplementary material[43]), meaning that the conformational composition reached a stationary state. This was characterized by approximately equal amounts of the two forms: 51% (*syn*):49% (*anti*).

In order to verify if this effect also works in the *anti* → *syn* direction, we have irradiated, once again, the matrix with NIR laser-light tuned at 6849 cm^{-1} in order to increase the concentration of the less stable *anti* form up to 73%, and let the sample for about half-an-hour at 30 K, periodically recording its mid-IR spectra. This resulted in a consumption of the less stable form, thus proving the bidirectional nature of this phenomenon.

The isothermal *syn* ↔ *anti* interconversion observed in the xenon matrix is most likely originated by the

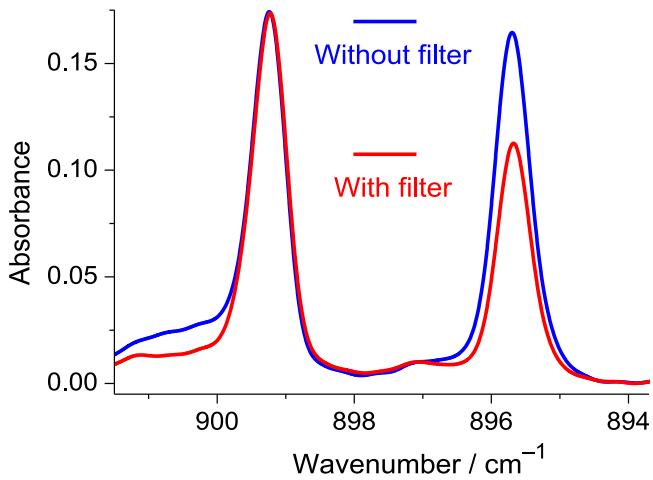

FIG. 7. Fragment of the spectrum of 6MOI isolated in a xenon matrix at 30 K, recorded immediately after deposition, in the presence of a filter transmitting only infrared light with wavenumbers below 2100 cm^{-1} (red) and in the absence of this filter (blue). The two spectra were normalized to the same peak intensity of the higher frequency band of the *syn* form.

NIR/mid-IR broadband radiation emitted from the source of the spectrometer, a type of photoeffect that has already been observed for systems differing by a flip of the OH group.[10,42] To confirm this, we have conducted another experiment in which the conformational composition of 6MOI in the xenon matrix during deposition was monitored by collecting only a part of IR spectrum. For this purpose, we used a cutoff IR filter placed between the spectrometer source and the matrix that blocks the sample from the IR light above 2200 cm^{-1}. This prevents the absorption by the molecule of energies higher than 26 kJ mol^{-1}. Figure 7 shows the spectral variations in the 899/896 cm^{-1} doublet resulting from the introduction of the filter. Clearly, the A_{syn}/A_{anti} ratio is much higher in the sample monitored with the presence of the filter than in the sample monitored without the filter. In quantitative terms and considering the contribution of all selected doublets, the abundances (mean values) of the two conformers in the matrix not exposed to the higher energy IR radiation emitted by the spectrometer source are estimated to be $P_{\text{syn}} \sim 68\%$:$P_{\text{anti}} \sim 32\%$.

From these results the following remarks can be made: (1) The broadband mid-IR radiation emitted by the spectrometer source is responsible for the interconversion between the two conformers in the xenon matrix at 30 K; (2) this effect shifts the conformational distribution towards a photostationary state characterized by nearly equal amounts of the two forms (on the time scale of hours); (3) the conformational distribution estimated after deposition of the xenon matrix with the filter is very close to the predicted MP2 gas-phase populations, thus indicating that the energy difference between the two conformers is predicted accurately enough by this theoretical method.

With the aim of checking whether the broadband IR radiation also affects the conformational distribution when the compound is isolated in solid argon, an additional experiment was performed. The matrix deposition, carried out at 16 K, was monitored by collecting spectra in the presence of the IR filter, which was removed upon completing deposition. Interestingly, after about 9 h of leaving the sample in the spectrometer beam, the recorded mid-IR spectrum was found to be practically coincident with that measured before removing the filter (see Figure S3 of the supplementary material[43]). Hence, contrarily to xenon, no conformational isomerization takes place in the argon matrix exposed to unfiltered radiation, difference that we attribute to the more tight trapping cages in the argon crystal lattice as compared to xenon. The abundances of the two conformers trapped in this host matrix ($P_{\text{syn}} \sim 67\%$:$P_{\text{anti}} \sim 33\%$) are equal to those estimated from the xenon spectra measured with the presence of the filter and to the MP2 gas-phase populations.

V. CONCLUSIONS

Conformational changes induced thermally or upon infrared excitation of matrix-isolated 6-methoxyindole were investigated. Narrowband infrared excitation of the first overtone of the N-H stretching vibration of each one of the two conformers (*syn*; *anti*) of the molecule induces the selective large-scale conversion of the pumped conformer into the other one. This allowed the full assignment of the infrared spectra of the conformers and to prepare matrices with different conformational compositions, which were subsequently used to investigate the effects of both thermal and broadband infrared excitations upon the conformational mixtures.

The results were substantially different in argon and xenon matrices:

- When argon is used as matrix medium, the gas phase conformational equilibrium prior to matrix preparation can be efficiently trapped in the matrix: for the used temperature of the 6MOI gas phase, 323 K, a *syn*:*anti* population ratio of about 2:1 was measured, matching well to the MP2 predicted population ratio at that temperature. Due to tight trapping cages in the argon solid lattice as compared to xenon, no conformational isomerization takes place in the argon matrix exposed to unfiltered broadband infrared radiation of the spectrometer beam.
- On the other hand, when xenon is used as host medium, the conformational composition existing in the gas phase can only be efficiently trapped in the matrix when the higher-energy infrared light (>2200 cm^{-1}) of the spectrometer beam is blocked during the experiments. Exposition of the sample to the unfiltered spectrometer infrared beam leads to IR-induced conformational interconversion. For a xenon matrix kept below the temperature at which the thermally induced *anti* → *syn* conversion becomes accessible (~35 K), prolonged exposition to the unfiltered spectrometer infrared beam leads to the attainment of a photostationary state with a population ratio of about 1:1, independently of the initial conformational composition of 6MOI in the matrix.

The effect of the unfiltered spectrometer infrared beam on the 6MOI conformational mixture also justifies the impossibility to completely depopulate the higher-energy *anti*

conformer upon annealing (at 50 K) of the xenon matrix of the compound exposed to the unfiltered spectrometer infrared beam during spectra collection. The different population ratio (about 1.5:1), measured immediately after deposition of the xenon matrix, compared to that observed both in case of the argon matrix and xenon matrix kept protected from radiation with $\lambda > 2200\ \mathrm{cm}^{-1}$, implies a partial *anti* → *syn* conversion, induced by the spectrometer light source.

Finally, it is important to emphasize that 6MOI, to the best of our knowledge, is the unique case where the isomerization of a heavy-atom fragment (methoxy group) takes place by the action of broad-band infrared and near-infrared light in a rigid matrix, in contrast to previous studies where electronic ground-state light-induced isomerizations were only related with the flip of light OH or SH groups.

ACKNOWLEDGMENTS

This work was supported by the Portuguese "Fundação para a Ciência e a Tecnologia" (FCT). The Coimbra Chemistry Centre is supported by the FCT through the Project No. PestOE/QUI/UI0313/2014. I.R. acknowledges FCT for the *Investigador FCT* grant.

[1]R. Fausto, L. Khriachtchev, and P. Hamm, in *Physics and Chemistry at Low Temperatures*, edited by L. Khriachtchev (Pan Stanford, Singapore, 2011), p. 51.
[2]A. J. Lopes Jesus, I. Reva, C. Araujo-Andrade, and R. Fausto, J. Am. Chem. Soc. **137**, 14240 (2015).
[3]A. Sharma, I. Reva, and R. Fausto, J. Am. Chem. Soc. **131**, 8752 (2009).
[4]M. Pettersson, J. Lundell, L. Khriachtchev, and M. Räsänen, J. Am. Chem. Soc. **119**, 11715 (1997).
[5]I. D. Reva, A. J. Lopes Jesus, M. T. S. Rosado, R. Fausto, M. Ermelinda Eusebio, and J. S. Redinha, Phys. Chem. Chem. Phys. **8**, 5339 (2006).
[6]M. T. S. Rosado, A. J. Lopes Jesus, I. D. Reva, R. Fausto, and J. S. Redinha, J. Phys. Chem. A **113**, 7499 (2009).
[7]I. D. Reva, S. Jarmelo, L. Lapinski, and R. Fausto, J. Phys. Chem. A **108**, 6982 (2004).
[8]G. Bazsó, E. E. Najbauer, G. Magyarfalvi, and G. Tarczay, J. Phys. Chem. A **117**, 1952 (2013).
[9]N. Akai, S. Kudoh, M. Takayanagi, and M. Nakata, J. Phys. Chem. A **106**, 11029 (2002).
[10]L. Lapinski, I. Reva, H. Rostkowska, R. Fausto, and M. J. Nowak, J. Phys. Chem. B **118**, 2831 (2014).
[11]E. E. Najbauer, G. Bazsó, S. Góbi, G. Magyarfalvi, and G. Tarczay, J. Phys. Chem. B **118**, 2093 (2014).
[12]S. Coussan, Y. Bouteiller, J. P. Perchard, and W. Q. Zheng, J. Phys. Chem. A **102**, 5789 (1998).
[13]S. Nishino and M. Nakata, J. Phys. Chem. A **111**, 7041 (2007).
[14]D. Gerbig and P. R. Schreiner, J. Phys. Chem. B **119**, 693 (2015).
[15]I. Reva, C. M. Nunes, M. Biczysko, and R. Fausto, J. Phys. Chem. A **119**, 2614 (2015).
[16]C. Seaiby, A. V. Zabuga, A. Svendsen, and T. R. Rizzo, J. Chem. Phys. **144**, 014304 (2016).
[17]T. R. Rizzo, J. A. Stearns, and O. V. Boyarkin, Int. Rev. Phys. Chem. **28**, 481 (2009).
[18]B. C. Dian, A. Longarte, and T. S. Zwier, J. Chem. Phys. **118**, 2696 (2003).
[19]B. C. Dian, A. Longarte, P. R. Winter, and T. S. Zwier, J. Chem. Phys. **120**, 133 (2004).
[20]B. C. Dian, J. R. Clarkson, and T. S. Zwier, Science **303**, 1169 (2004).
[21]A. Halasa, L. Lapinski, H. Rostkowska, and M. J. Nowak, J. Phys. Chem. A **119**, 9262 (2015).
[22]C. M. Nunes, L. Lapinski, R. Fausto, and I. Reva, J. Chem. Phys. **138**, 125101 (2013).
[23]A. Halasa, L. Lapinski, I. Reva, H. Rostkowska, R. Fausto, and M. J. Nowak, J. Phys. Chem. A **119**, 1037 (2015).
[24]N. Kuş, A. Sharma, I. Reva, L. Lapinski, and R. Fausto, J. Phys. Chem. A **114**, 7716 (2010).
[25]S. Breda, I. Reva, L. Lapinski, and R. Fausto, J. Phys. Chem. A **110**, 11034 (2006).
[26]N. Kaushik, N. Kaushik, P. Attri, N. Kumar, C. Kim, A. Verma, and E. Choi, Molecules **18**, 6620 (2013).
[27]R. Vicente, Org. Biomol. Chem. **9**, 6469 (2011).
[28]A. J. Kochanowska-Karamyan and M. T. Hamann, Chem. Rev. **110**, 4489 (2010).
[29]S. Mahboobi, H. Pongratz, H. Hufsky, J. Hockemeyer, M. Frieser, A. Lyssenko, D. H. Paper, J. Bürgermeister, F.-D. Böhmer, H.-H. Fiebig, A. M. Burger, S. Baasner, and T. Beckers, J. Med. Chem. **44**, 4535 (2001).
[30]G. Tarzia, G. Diamantini, B. Di Giacomo, G. Spadoni, D. Esposti, R. Nonno, V. Lucini, M. Pannacci, F. Fraschini, and B. M. Stankov, J. Med. Chem. **40**, 2003 (1997).
[31]A. D. Becke, Phys. Rev. A **38**, 3098 (1988).
[32]C. T. Lee, W. T. Yang, and R. G. Parr, Phys. Rev. B **37**, 785 (1988).
[33]S. H. Vosko, L. Wilk, and M. Nusair, Can. J. Phys. **58**, 1200 (1980).
[34]C. Møller and M. S. Plesset, Phys. Rev. **46**, 618 (1934).
[35]M. J. Frisch, G. W. Trucks, H. B. Schlegel, G. E. Scuseria, M. A. Robb, J. R. Cheeseman, G. Scalmani, V. Barone, B. Mennucci, G. A. Petersson, H. Nakatsuji, M. Caricato, X. Li, H. P. Hratchian, A. F. Izmaylov, J. Bloino, G. Zheng, J. L. Sonnenberg, M. E. M. Hada, K. Toyota, R. Fukuda, J. Hasegawa, M. Ishida, T. Nakajima, Y. Honda, O. Kitao, H. Nakai, T. Vreven, J. A. Montgomery, Jr., J. E. Peralta, F. Ogliaro, M. Bearpark, J. J. Heyd, E. Brothers, K. N. Kudin, V. N. Staroverov, R. Kobayashi, J. Normand, K. Raghavachari, A. Rendell, J. C. Burant, S. S. Iyengar, J. Tomasi, M. Cossi, N. Rega, J. M. Millam, M. Klene, J. E. Knox, J. B. Cross, V. Bakken, C. Adamo, J. Jaramillo, R. Gomperts, R. E. Stratmann, O. Yazyev, A. J. Austin, R. Cammi, C. Pomelli, J. W. Ochterski, R. L. Martin, K. Morokuma, V. G. Zakrzewski, G. A. Voth, P. Salvador, J. J. Dannenberg, S. Dapprich, A. D. Daniels, Ö. Farkas, J. B. Foresman, J. V. Ortiz, J. Cioslowski, and D. J. Fox, GAUSSIAN 09, Revision D.01, Gaussian, Inc., Wallingford, CT, 2009.
[36]A. J. Lopes Jesus and J. S. Redinha, Struct. Chem. **26**, 655 (2015).
[37]C. Brand, O. Oeltermann, M. Wilke, and M. Schmitt, J. Chem. Phys. **138**, 024321 (2013).
[38]P. Felder and H. H. Günthard, Chem. Phys. **71**, 9 (1982).
[39]A. J. Barnes, J. Mol. Struct. **113**, 161 (1984).
[40]It should be noted that the theoretically predicted frequencies of the NH stretching mode coincide within one wavenumber (see Table II). The ordering of these peaks appearing in the experiments depends on fine interactions between the isolated 6MOI monomers and the matrix host gas. In a Xe matrix, the NH stretching band assigned to the most stable form appears at a slightly higher frequency relative to the absorption assigned to the less stable conformer. In an argon matrix, the guest:host interactions are similar for both conformers, and combined with manifestations of different matrix sites, the respective absorption components of the anti and syn forms appear interlaced.
[41]I. Reva, A. Simão, and R. Fausto, Chem. Phys. Lett. **406**, 126 (2005).
[42]I. Reva, M. J. Nowak, L. Lapinski, and R. Fausto, J. Chem. Phys. **136**, 064511 (2012).
[43]See supplementary material at http://dx.doi.org/10.1063/1.4944528 for optimized Cartesian coordinates and calculated infrared spectra of the two 6MOI conformers, as well as for the changes in spectra of matrix-isolated 6MOI after annealing and absence of changes in the spectra upon long exposure to the spectrometer light source.